arXiv:1302.1818v1 [cond-mat.str-el] 7 Feb 2013

Ferromagnetic Anisotropy from Antiferromagnetic Superexchange in the Mixed $3d-5d$ Transition-Metal Compound Sr_3CuIrO_6

Wei-Guo Yin,[1,*] X. Liu,[2,1] A. M. Tsvelik,[1] M. P. M. Dean,[1] M. H. Upton,[3]
Jungho Kim,[3] D. Casa,[3] A. Said,[3] T. Gog,[3] T. F. Qi,[4,5] G. Cao,[4,5] and J. P. Hill[1]
[1]*Condensed Matter Physics and Materials Science Department,*
Brookhaven National Laboratory, Upton, New York 11973, USA
[2]*Beijing National Laboratory for Condensed Matter Physics,*
and Institute of Physics, Chinese Academy of Sciences, Beijing 100190, China
[3]*Advanced Photon Source, Argonne National Laboratory, Argonne, Illinois 60439, USA*
[4]*Center for Advanced Materials, University of Kentucky, Lexington, Kentucky 40506, USA*
[5]*Department of Physics and Astronomy, University of Kentucky, Lexington, Kentucky 40506, USA*
(Dated: February 8, 2013)

We report a combined experimental and theoretical study of the unusual ferromagnetism in the quasi-one-dimensional copper-iridium oxide Sr_3CuIrO_6. Utilizing Ir L_3 edge resonant inelastic x-ray scattering, we reveal a large gap magnetic excitation spectrum, and show that it is well described by the $S = 1/2$ Heisenberg model with an Ising-like ferromagnetic exchange anisotropy. We present a microscopic derivation of this model and find an unexpected effect, namely the ferromagnetic anisotropy arises from the antiferromagnetic superexchange interaction, driven by the alternating strong and weak spin-orbit coupling on the Ir and Cu magnetic ions, respectively. Our results point to the unusual magnetic behavior to be expected in mixed $3d-5d$ transition-metal compounds via exchange pathways that are absent in pure $3d$ or $5d$ compounds.

PACS numbers: 75.30.Et, 71.70.Ej, 78.70.Ck, 75.10.Dg

The interest in strongly correlated electronic systems has recently been extended from $3d$ transition-metal compounds (TMCs) to $5d$ compounds. Usually the strength of electron correlation is characterized by the ratio of the local Coulomb repulsion to the electronic bandwidth. A large value of this ratio (~ 8) is common in $3d$ TMCs such as superconducting cuprates [1]. Since $5d$ orbitals are more extended in space and host weaker Coulomb interactions than $3d$ orbitals, $5d$ TMCs are generally expected to be weakly correlated. However, it has been pointed out [2–4] that the relative weakness of the Coulomb interaction is offset by the strong spin-orbit coupling (SOC), which is typically ~ 0.5 eV for $5d$ elements. This strong SOC leads to a significant splitting and narrowing of the electronic bands, and pushes $5d$ TMCs toward the strongly correlated regime. Indeed, the SOC-driven Mott metal-insulator transition was shown to exist in a variety of $5d$ iridium oxides [2–14]. An important consequence is the entanglement of the orbital and spin degrees of freedom in the resulting localized magnetic moments (termed as 'isospins'), which can lead to unusual superexchange pathways and to new physics, for example, the proposed spin-liquid state as encoded in the Kitaev model [15] in the honeycomb-lattice $(Li,Na)_2IrO_3$ [7] and possible superconductivity in the square-lattice Sr_2IrO_4, which shows a similar magnetic ordering and dynamics to the cuprates [5].

The purpose of this letter is to demonstrate that materials containing *both* $3d$ and $5d$ magnetic ions can host new physics absent in either pure $3d$ or pure $5d$ compounds - because of the unique combination of unusual exchange pathways and special geometries, a result of the strong SOC of the $5d$ electrons and the differing coordinations of the $3d$ and $5d$ sites. Such materials will offer new avenues to engineer exotic magnetic behavior. To demonstrate this, we have chosen to study the quasi-one-dimensional copper-iridium oxide, Sr_3CuIrO_6, as a prototype for such mixed $3d-5d$ systems. The crystal structure of this compound (Fig. 1) is reminiscent of both the superconducting cuprates and iridium-based Mott insulators: Specifically, it contains with the chains of alternating Cu and Ir the Cu^{2+} in a planar oxygen coordination and the Ir^{4+} in an octahedral oxygen coordination . The physical novelty of this material is demonstrated by the emergence of ferromagnetic order, which is rare in pure cuprates or iridates (the closely related materials Sr_3CuPtO_6 and Sr_3ZnIrO_6 are antiferromagnetic) [16, 17]. There is to date no microscopic understanding of this unique phenomenon.

Here we use Ir L_3 edge resonant inelastic x-ray scattering (RIXS) to reveal a large gap magnetic excitation spectrum, and show that it is well described by the effective $S = 1/2$ Heisenberg model with an Ising-like ferromagnetic exchange anisotropy. We present a microscopic derivation of this model, and find that the arrangement of alternating isospins and real spins on the Ir-Cu chain leads to an unexpected effect, namely that the ferromagnetic anisotropy arises from the antiferromagnetic superexchange. Our results point to an entirely new class of magnetic behavior in mixed $3d-5d$ TMCs.

RIXS measurements.—The energy and momentum dependence of the magnetic excitation spectrum in a self-

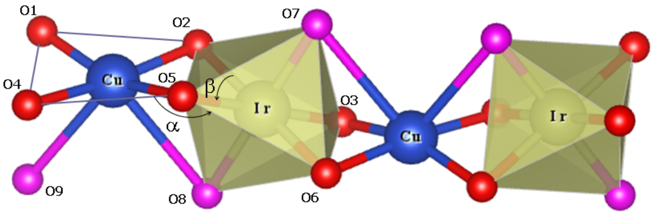

FIG. 1. Cu-Ir chain of Sr_3CuIrO_6 where Cu^{2+} and Ir^{4+} are coordinated by an oxygen plaquette and octahedron, respectively. The IrO_6 octahedral tilting is denoted by $\alpha \simeq 150°$ and the octahedral distortion by $\beta \simeq 82°$.

flux-grown Sr_3CuIrO_6 single crystal was studied by using Ir L_3 edge RIXS, for which dipole transitions excite and deexcite a $2p_{3/2}$ core-electron to the $5d$ orbitals [18]. The measurements were carried out at beamline 9-ID, Advanced Photon Source, in a horizontal scattering geometry. A Si(844) secondary monochromator and a R=2m Si(844) diced analyzer were utilized. The overall energy resolution of this setup was ~ 45 meV (FWHM) and the momentum resolution was better than 0.07 of the Brillouin zone (BZ) length along the Cu-Ir chain direction. All data were collected at 7 K.

Fig. 2(a) shows the low-energy RIXS spectra for the momentum transfer q along the chain direction in the BZ in which the unit cell contains one Cu ion and one Ir ion. A shoulder appears near the elastic line and disperses along the chain direction. No dispersion is seen in this feature for momentum transfers perpendicular to the chain direction (not shown). We attribute this shoulder to a one-dimensional magnon mode. Its dispersion is plotted in Fig. 2(b), and shows two salient features: (i) The minimum energy located at the Γ point is not zero, but rather shows a large gap of ~ 30 meV, comparable to the magnon bandwidth. (ii) The dispersive behavior follows the periodicity of the (one Ir plus one Cu) chain unit cell very well, approximately in the form of $\cos(qa)$ where a is the nearest Ir-Ir distance.

These observations cannot be explained by conventional models. The simple linear chain ferromagnetic Heisenberg model proposed for this system [16] is gapless. In the related iridate Sr_3ZnIrO_6, two mechanisms have been proposed for a possible gap there. However, neither can be at work here. In the first, singlet dimers were proposed based on the alternating chain antiferromagnetic Heisenberg model [17]. However, this cannot occur in Sr_3CuIrO_6, since it is ferromagnetic. In the second, an Ising-like exchange anisotropy is added to the $S = 1/2$ Heisenberg model [19]. However, the magnon dispersion of the ferromagnetic model of this type, in which one does not distinguish between Cu and Ir atoms (i.e., the unit cell contains one magnetic ion), is in the form of $\cos(qa/2)$ [20, 21], in disagreement with the dispersion observed above. Our data thus require unconventional magnetism in this system, and make a general call for a new understanding of systems with mixed $3d - 5d$ magnetic ions.

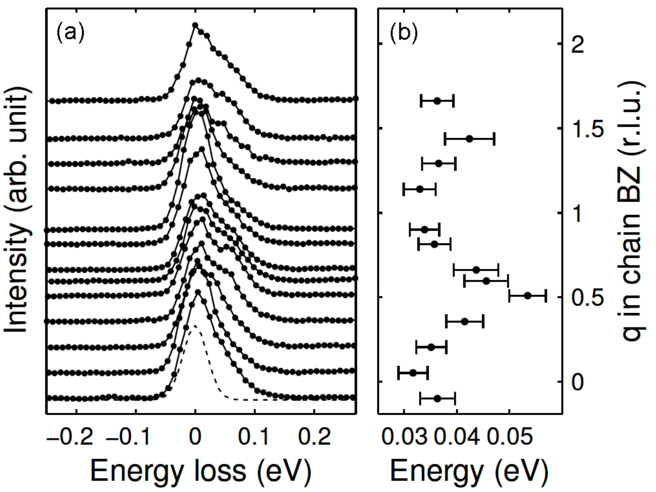

FIG. 2. (a) RIXS spectra for different momentum transfer along the chain direction, compared with the off-resonant elastic line (dotted line). (b) the extracted magnetic dispersion from the scans shown in (a). The scans in (a) are offset to match with their wavevector transfer along the chain direction presented in (b).

Microscopic mechanism.—To understand the microscopic origin of the Mottness, the ferromagnetism, and the anisotropy in this system, we start by analyzing the geometry and symmetry of the Cu-Ir chain.

A portion of a Cu-Ir chain of Sr_3CuIrO_6 is shown in Fig. 1. The Cu^{2+} ion is located at the center of an oxygen plaquette. The only magnetic orbital ϕ_{Cu} centered on a Cu^{2+} ion is of $x^2 - y^2$ symmetry and is antisymmetric with regard to the Cu-Ir mirror plane [22].

By contrast, the Ir^{4+} ion lies in the center of an oxygen octahedron which shares an edge with neighboring CuO_4 plaquettes and experiences tilting and an orthorhombic distortion characterized by angles $\alpha \simeq 150°$ and $\beta \simeq 82°$, respectively, as defined in Fig. 1. The octahedral ligand field renders the three Ir t_{2g} ($5d_{xy}$, $5d_{xz}$, and $5d_{yz}$) orbitals relevant to the low-energy physics, while the two unoccupied Ir e_g energy levels are ~ 3 eV higher [14]. We shall show below that the octahedral tilting and distortion are also relevant to the magnetism in Sr_3CuIrO_6, and that the role of the Ir $5d_{xy}$ orbital is completely different from those of the Ir $5d_{xz}$ and $5d_{yz}$ orbitals.

The Ir $5d_{xy}$ orbital, $\phi_{\mathrm{Ir},xy}$, is symmetric with regard to the Cu-Ir mirror plane, even in the presence of the octahedral tilting and distortion. Thus, $\phi_{\mathrm{Ir},xy}$ is always orthogonal to ϕ_{Cu}. As a result, electron hopping between these two orbitals is prohibited and so is the superexchange process. Thus, the leading magnetic interaction between them is the direct exchange interaction, J_{F}, which is ferromagnetic [23, 24]. From the measured magnon bandwidth (Fig. 2), we conclude that J_{F} is of order of dozens of meV. This is surprising, since direct exchange in TMCs is usually very small. The unusually large J_{F} comes from the fact that the tails of $\phi_{\mathrm{Ir},xy}$ and ϕ_{Cu} actually overlap well around each of O2 and O5 in Fig. 1 but with opposite sign [22], similar to the large direct exchange ferromagnetism proposed for a Cu^{2+}-$(\mathrm{VO})^{2+}$ heterobinuclear complex [25].

The Ir $5d_{xz}/5d_{yz}$ orbitals are also orthogonal to ϕ_{Cu} for the ideal case of $\alpha = 180°$ and $\beta = 90°$. Therefore, the electron hopping and superexchange between them are also prohibited. However, the realistic octahedral tilting immediately breaks the orthogonality of the Ir $5d_{xz}/5d_{yz}$ orbitals and ϕ_{Cu}, and induces electron hopping between them. It is reasonable to expect this tilting induced kinematic process to be weak and to contribute an antiferromagnetic superexchange. Thus, the material is a Mott insulator accounting for the validity of the isolated IrO_6 octahedron model for the $d-d$ charge excitations [14]. On the other hand, in sharp contrast with the Ir $5d_{xy}$ orbital, the Ir $5d_{xz}$ ($5d_{yz}$) orbital has a tail of p_z symmetry around O2 (O5), which leads to a vanishing overlap, and thus a vanishing direct exchange, with the ϕ_{Cu} regardless of the octahedral tilting. Therefore, the leading magnetic interaction between the Ir $5d_{xz}/5d_{yz}$ orbitals and ϕ_{Cu} is the antiferromagnetic superexchange.

The above considerations lead to the following effective Hamiltonian describing the magnetic interactions in $\mathrm{Sr}_3\mathrm{CuIrO}_6$:

$$\begin{aligned} H = \quad & -J_{\mathrm{F}} \sum_{\langle \mathbf{m},\mathbf{n}\rangle} \vec{S}_{\mathbf{m},x^2-y^2} \cdot \vec{S}_{\mathbf{n},xy} \\ & + J_{\mathrm{AF}} \sum_{\langle \mathbf{m},\mathbf{n}\rangle} \vec{S}_{\mathbf{m},x^2-y^2} \cdot (\vec{S}_{\mathbf{n},yz} + \vec{S}_{\mathbf{n},zx}) \\ & + \lambda \sum_{\mathbf{n}} \vec{L}_{\mathbf{n}} \cdot \vec{S}_{\mathbf{n}} \\ & + \Delta \sum_{\mathbf{n}\sigma} d^{\dagger}_{\mathbf{n},xy,\sigma} d_{\mathbf{n},xy,\sigma}, \end{aligned} \tag{1}$$

where $\mathbf{m}$ denotes a Cu site, $\mathbf{n}$ an Ir site, and $\langle \mathbf{m},\mathbf{n}\rangle$ means nearest neighbors. $\vec{S}_{\mathbf{n},\gamma} = \sum_{\mu\nu} d^{\dagger}_{\mathbf{n},\gamma,\mu} \vec{\sigma}_{\mu\nu} d_{\mathbf{n},\gamma,\nu}/2$ where $\vec{\sigma}_{\mu\nu}$ is the Pauli matrix and $d_{\mathbf{n},\gamma,\mu}$ is the annihilation operator of an electron with spin $\mu = \uparrow, \downarrow$ and orbital $\gamma = xy, xz, yz$ on the Ir site $\mathbf{n}$. $-J_{\mathrm{F}} < 0$ is the ferromagnetic direct exchange coupling between the Ir $5d_{xy}$ and Cu $3d_{x^2-y^2}$ orbitals. $J_{\mathrm{AF}} > 0$ is the antiferromagnetic superexchange coupling between the Ir $5d_{xz}/5d_{yz}$ and Cu $3d_{x^2-y^2}$ orbitals, which is nonzero in the presence of IrO_6 octahedral tilting. $\lambda = 0.44$ eV is the SOC constant on the Ir sites, and $\Delta = 0.31$ eV is the strength of the orthorhombic distortion of the IrO_6 octahedra [14].

Here we focus on energy scales for which only one hole can occupy a given site, as the system is in the clean limit of a Mott insulator. The remaining leading energy scales are λ and Δ, which split the local energy levels on the Ir site into three doublets with the lowest one clearly separated from the others [14]. The lowest-energy doublet is of the form [22]

$$|\phi_{0,\eta}\rangle = \frac{1}{\sqrt{2+p^2}} (p d_{xy,\eta} + \mathrm{i} d_{yz,\bar{\eta}} + \eta d_{zx,\bar{\eta}}), \quad \eta = \pm, \tag{2}$$

where $p = 0, 1$ for $\Delta = \infty, 0$, respectively. Retaining only $|\phi_{0,\eta}\rangle$ in second-order perturbation theory, we arrive at the following effective $S = 1/2$ Hamiltonian [22]:

$$\begin{aligned} H_{\mathrm{eff}} = & -J_1 \sum_{\langle \mathbf{m},\mathbf{n}\rangle} \left\{ S^x_{\mathbf{m}} s^x_{\mathbf{n}} + S^y_{\mathbf{m}} s^y_{\mathbf{n}} + \gamma_1 S^z_{\mathbf{m}} s^z_{\mathbf{n}} \right\} \\ & - J_2 \sum_{\langle\langle \mathbf{m},\mathbf{m}'\rangle\rangle} \left\{ S^x_{\mathbf{m}} S^x_{\mathbf{m}'} + S^y_{\mathbf{m}} S^y_{\mathbf{m}'} + \gamma_2 S^z_{\mathbf{m}} S^z_{\mathbf{m}'} \right\}, \end{aligned} \tag{3}$$

where $\langle \mathbf{m},\mathbf{n}\rangle$ and $\langle\langle \mathbf{m},\mathbf{m}'\rangle\rangle$ mean the nearest Cu-Ir and Cu-Cu neighbors, respectively. $\vec{s}_{\mathbf{n}} = \sum_{\eta\eta'} |\phi_{0,\eta}\rangle \vec{\sigma}_{\eta\eta'} \langle \phi_{0,\eta'}|/2$ is the isospin on the Ir site. The parameters are

$$\begin{aligned} J_1 &= J_{\mathrm{F}} \frac{p^2}{2+p^2} > 0, \\ \gamma_1 &= 1 + \frac{2\epsilon}{p^2} > 1, \text{where } \epsilon = J_{\mathrm{AF}}/J_{\mathrm{F}} > 0, \\ J_2 &= \left(\frac{J_{\mathrm{F}}}{4+2p^2} \right)^2 \left(\frac{4(2+p^2)\epsilon^2}{E_1 - E_0} + \frac{4p^2}{E_2 - E_0} \right) > 0, \\ \gamma_2 &= \frac{(1-\epsilon)^2}{1 + (1 + \frac{2}{p^2})\epsilon^2 \frac{E_2 - E_0}{E_1 - E_0}} < 1, \end{aligned} \tag{4}$$

where $E_2 - E_0 = 0.81$ eV and $E_1 - E_0 = 0.58$ eV are local energy splitting on the Ir site [14]. The result is an extended ferromagnetic XXZ model with the J_1 terms making up the regular chain model with easy-axis anisotropy ($\gamma_1 > 1$) and the additional J_2 terms with easy-plane anisotropy ($\gamma_2 < 1$) appearing only for the Cu sites.

What is remarkably new here is that the ferromagnetic anisotropy, $\gamma_1 - 1 = (2/p^2) J_{\mathrm{AF}}/J_{\mathrm{F}}$, originates from the

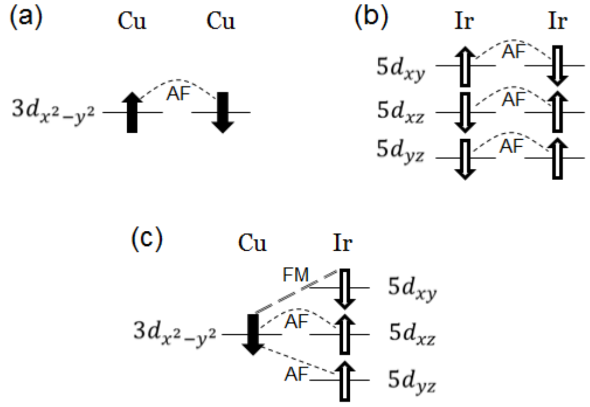

FIG. 3. Schematics of three different exchange pathways: (a) between Cu $3d_{x^2-y^2}$ orbitals in $\mathrm{La}_2\mathrm{CuO}_4$, (b) between Ir $5d$ orbitals in $\mathrm{Sr}_2\mathrm{IrO}_4$ (open arrows mean partial occupation in the $j = 1/2$ state, $|\phi_{0,\pm}\rangle$), and (c) between Cu $3d_{x^2-y^2}$ and Ir $5d$ orbitals in $\mathrm{Sr}_3\mathrm{CuIrO}_6$. Dashed lines indicate the exchange type: antiferromagnetic (AF) or ferromagnetic (FM).

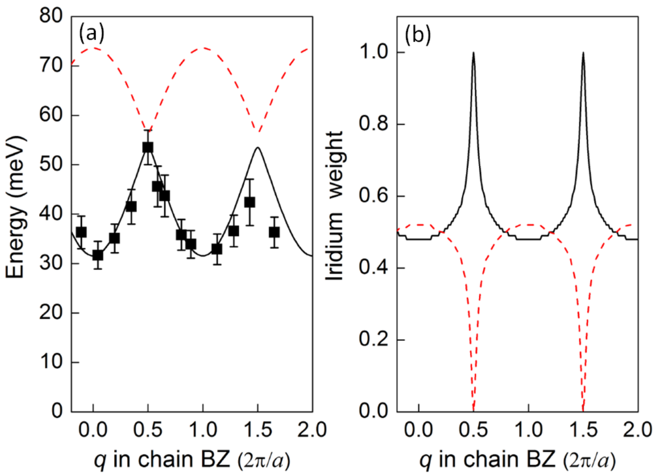

FIG. 4. (a) Calculated magnon dispersion (lines), compared with the experimental data (solid squares). (b) The Ir partial spectral weights for the lower (solid line) and upper (dashed line) branches in (a). $J_1 = 21$ meV, $\gamma_1 J_1 = 53.5$ meV, $J_2 = 2.4$ meV, $\gamma_2 J_2 = 0.6$ meV are used.

antiferromagnetic exchange between the Ir $5d_{xz}/5d_{yz}$ and Cu $3d_{x^2-y^2}$ orbitals. The difference of this unusual exchange pathway from those in the cuprate La_2CuO_4 and the iridate Sr_2IrO_4 [7] is illustrated in Fig. 3. The present finding can be understood by looking closely at $|\phi_{0,\eta}\rangle$ [Eq. (2)], in which the Ir $5d_{xy}$ and $5d_{xz}/5d_{yz}$ orbitals have opposite spin orientations. Therefore, the tendency of the spin in the Ir $5d_{xy}$ ($5d_{xz}/5d_{yz}$) orbital to be parallel (antiparallel) to neighboring Cu spins can be satisfied simultaneously via this spin-orbital-coupled Kramers doublet [c.f., Fig. 3(c)], yielding the antiferromagnetism-induced ferromagnetic anisotropy. The Ir $5d_{xz}$ and $5d_{yz}$ orbitals contribute only to the diagonal part of H_{eff} because their contributions to the off-diagonal part cancel out each other. The reduction of p from unity by the realistic octahedral distortion ($\Delta > 0$) will significantly enhance the anisotropy and reduce J_1, because those changes are related to p^2. This will substantially increase the gap size and reduce the magnon bandwidth. It is noteworthy that in the context of the Kitaev model, an Ising-like ferromagnetic exchange anisotropy due to the simultaneous presence of SOC and Hund's rule coupling was suggested for $(Li,Na)_2IrO_3$ [7]. We emphasize that the present mechanism for creating such an anisotropy is entirely different because it is independent of Hund's rule coupling.

The Hamiltonian of Eq. (3) with $J_2 = 0$ is integrable [20, 21]. Its spectrum consists of a fundamental magnon mode and multi-magnon bound states. The single magnon dispersion is $\omega(q) = J_1[\gamma_1 - \cos(qa/2)]$, where a is the nearest Ir-Ir distance and q a momentum along the Cu-Ir chain. This expression coincides with the spin-wave dispersion calculated using the Holstein-Primakoff transformation. For $J_2 \neq 0$ the latter method yields [22]:

$$\omega_{\mp}(q) = \frac{1}{2}[2\gamma_1 J_1 + \gamma_2 J_2 - J_2\cos(qa)] \mp \frac{1}{2}\sqrt{[\gamma_2 J_2 - J_2\cos(qa)]^2 + 4J_1^2\cos^2(qa/2)}.$$

The second-neighbor interaction opens another gap of size $(1+\gamma_2)J_2$ at $q = \pi/a$ in the middle of the band. The lower branch $\omega_-(q)$ can be fit in good agreement to the experimental data, as shown in Fig. 4(a), for $J_1 = 21$ meV, $\gamma_1 J_1 = 53.5$ meV, $J_2 = 2.4$ meV, and $\gamma_2 J_2 = 0.6$ meV, which satisfy the theory constraints given by Eq. (4). From these numbers together with $\lambda = 0.44$ eV and $\Delta = 0.31$ eV [14] we extract estimates $J_{\text{F}} = 120$ meV and $J_{\text{AF}} = 39$ meV.

This raises the question as to why the upper branch $\omega_+(q)$ is missing in our RIXS measurement. It is possible that the upper-branch magnons decay into an energy continuum, as this material is close to a spin glass [26]. Another likely explanation is that because the data were taken at the Ir L_3 edge, only the Ir weight is visible in the present observation. The weights of Ir character [22] in the lower (-) and upper (+) branch of the spin-wave dispersion, $I_{\mp}(q)$, are shown in Fig. 4(b). $I_-(q)$ (solid line) is generally much larger than $I_+(q)$ (dashed line) and it follows the chain BZ, in agreement with the RIXS data. Note that $I_{\mp}(q) \equiv 1/2$ for $J_2 = 0$; it is interesting that a tiny J_2 ($J_2/J_1 \sim 0.1$) dramatically changes the weight distribution. By the sum rule the Cu partial spectral weight is $1 - I_{\mp}(q)$, and therefore $\omega_+(q)$ should be detectable by Cu L_3 edge RIXS [27] and this will be pursued in the feature [28].

In summary, we have presented a combined experimental and theoretical study of the unusual ferromagnetism in Sr_3CuIrO_6. We find that the peculiar geometry of the Cu-Ir chain facilitates a clean Mott insulator state and a strikingly large ferromagnetic direct exchange between the Ir $5d_{xy}$ and Cu $3d_{x^2-y^2}$ orbitals, while the octahedral tilting induces antiferromagnetic superexchange between the Ir $5d_{xz}/5d_{yz}$ and Cu $3d_{x^2-y^2}$ orbitals. These seemingly incompatible magnetic interactions work cooperatively, via the spin-orbital-coupled low-energy Kramers doublet on the Ir site, to yield respectively the isotropic and anisotropic parts of the ferromagnetism in Sr_3CuIrO_6. Our results demonstrate that mixed $3d-5d$ compounds can generate distinct exchange pathways and thus novel magnetic behavior that are absent in pure $3d$ or $5d$ compounds.

The work at Brookhaven National Laboratory was supported by the U.S. Department of Energy (DOE), Division of Materials Science, under Contract No. DE-AC02-98CH10886. Use of the Advanced Photon Source was supported by DOE, Office of Science, Office of Basic Energy Sciences, under Contract No. DE-AC02-06CH11357. T.F.Q and G.C. were supported by the NSF through grant No. DMR-0856234.

---

* wyin@bnl.gov

[1] E. Dagotto, Science, **309**, 257 (2005).

[2] B. J. Kim, H. Ohsumi, T. Komesu, S. Sakai, T. Morita, H. Takagi, and T. Arima, Science, **323**, 1329 (2009).

[3] B. J. Kim, H. Jin, S. J. Moon, J.-Y. Kim, B.-G. Park, C. S. Leem, J. Yu, T. Noh, C. Kim, S.-J. Oh, J.-H. Park, V. Durairaj, G. Cao, and E. Rotenberg, Phys. Rev. Lett., **101**, 076402 (2008).

[4] S. J. Moon, H. Jin, K. Kim, W. S. Choi, Y. S. Lee, J. Yu, G. Cao, A. Sumi, H. Funakubo, C. Bernhard, and T. Noh, Phys. Rev. Lett., **101**, 226402 (2008).

[5] J. Kim, D. Casa, M. H. Upton, T. Gog, Y.-J. Kim, J. F. Mitchell, M. van Veenendaal, M. Daghofer, J. van den Brink, G. Khaliullin, and B. J. Kim, Phys. Rev. Lett., **108**, 177003 (2012).

[6] D. Pesin and L. Balents, Nature Phys., **6**, 376 (2010).

[7] G. Jackeli and G. Khaliullin, Phys. Rev. Lett., **102**, 017205 (2009).

[8] Y. Singh, S. Manni, J. Reuther, T. Berlijn, R. Thomale, W. Ku, S. Trebst, and P. Gegenwart, Phys. Rev. Lett., **108**, 127203 (2012).

[9] X. Liu, T. Berlijn, W.-G. Yin, W. Ku, A. Tsvelik, Y.-J. Kim, H. Gretarsson, Y. Singh, P. Gegenwart, and J. P. Hill, Phys. Rev. B, **83**, 220403(R) (2011).

[10] S. K. Choi, R. Coldea, A. N. Kolmogorov, T. Lancaster, I. I. Mazin, S. J. Blundell, P. G. Radaelli, Y. Singh, P. Gegenwart, K. R. Choi, S.-W. Cheong, P. J. Baker, C. Stock, and J. Taylor, Phys. Rev. Lett., **108**, 127204 (2012).

[11] F. Ye, S. Chi, H. Cao, B. C. Chakoumakos, J. A. Fernandez-Baca, R. Custelcean, T. F. Qi, O. B. Korneta, and G. Cao, Phys. Rev. B, **85**, 180403(R) (2012).

[12] J. Kim, Y. Choi, J. Kim, J. F. Mitchell, G. Jackeli, M. Daghofer, J. van den Brink, G. Khaliullin, and B. J. Kim, Phys. Rev. Lett., **109**, 037204 (2012).

[13] R. Arita, J. Kuneš, A. Kozhevnikov, A. G. Eguiluz, and M. Imada, Phys. Rev. Lett., **108**, 086403 (2012).

[14] X. Liu, V. M. Katukuri, L. Hozoi, W.-G. Yin, M. P. M. Dean, M. H. Upton, J. Kim, D. Casa, A. Said, T. Gog, T. Qi, G. Cao, A. M. Tsvelik, J. van den Brink, and J. P. Hill, Phys. Rev. Lett., **109**, 157401 (2012).

[15] A. Kitaev, Ann. Phys. (N.Y.), **321**, 2 (2006).

[16] T. N. Nguyen, P. A. Lee, and H.-C. zur Loye, Science, **271**, 489 (1996).

[17] T. N. Nguyen and H.-C. zur Loye, J. Solid State Chem., **117**, 300 (1995).

[18] L. J. Ament, M. van Veenendaal, T. P. Devereaux, J. P. Hill, and J. van den Brink, Rev. Mod. Phys., **83**, 705 (2011).

[19] C. Lampe-Önnerud, M. Sigrist, and H.-C. zur Loye, J. Solid State Chem., **127**, 25 (1996).

[20] C. N. Yang and C. P. Yang, Phys. Rev., **151**, 258 (1966).

[21] J. D. Cloizer and M. Gaudin, J. Math. Phys., **7**, 1384 (1966).

[22] See Supplementary Material at [http://link.aps.org/supplemental/xxxxxxxxx] for technical details.

[23] J. Kanamori, J. Phys. Chem. Solids, **10**, 87 (1959).

[24] P. W. Anderson, Phys. Rev., **79**, 350 (1950).

[25] O. Kahn, J. Galy, Y. Journaux, J. Jaud, and I. Morgenstern-Badarau, J. Am. Chem. Soc., **104**, 2165 (1982).

[26] A. Niazi, E. V. Sampathkumaran, P. L. Paulose, D. Eckert, A. Handstein, and K.-H. Müller, Phys. Rev. B, **65**, 064418 (2002).

[27] M. P. M. Dean, R. S. Springell, C. Monney, K. J. Zhou, J. Pereiro, I. Božović, B. D. Piazza, H. M. Rnnow, E. Morenzoni, J. van den Brink, T. Schmitt, and J. P. Hill, Nature Mater., **11**, 850 (2012).

[28] To date, the energy resolution of Cu L_3 edge RIXS is about 130 meV for practical use, which is not good enough to discern the magnetic excitations $\sim$ 60 meV in this material. Facilities expected to operate with 10 meV resolution are under construction, for example, at Brookhaven National Laboratory as part of NSLS II.